A Novel Technique for Modelling Ship Magnetic Signatures

Carmen E. Lucas and Troy C. Richards

Defence Research and Development Canada

June 18, 2015

Abstract

This paper presents a new technique for modelling the magnetic signature of a naval platform. Recorded magnetic measurements of a ship's signature are transformed into a three-axis rectangular coordinate system relative to the vessel, which facilitates the modelling of the ship's magnetic signature using a distribution of longitudinal prolate spheroids with magnetizations in three dimensions. A unique magnetic inversion technique known as one-spike-at-a-time is used to generate an optimally sparse set of model magnetizations that fit the measured data and permit the rapid visualization of the vessel's magnetic signature anywhere in space, and is particularly useful for reporting signature levels at standardized depths and offsets. The model based signature approach simplifies signature manipulation such as the separation of the permanent and induced magnetic signature, and is demonstrated using magnetic north and south runs recorded for CFAV Quest.

1. Introduction

Since World War II, Navies around the world have been concerned with the magnetic mine threat and have taken action to reduce their vessels' signatures and, therefore, the risk. The measurement of underwater magnetic signatures is the first step to understanding, and ultimately developing countermeasures to decrease the signature. Through the latter part of the twentieth-century most Navies developed magnetic ranges based on induction coils which were mounted on the seafloor and surveyed into position. The induction coils were arranged in a three-axis configuration and each sensor coil was connected to shore by a twisted pair cable where the signal was amplified and digitally recorded. The coils were typically aligned to magnetic north-south, and magnetic east-west, and the ship transited in straight tracks perpendicular to the sensor line.

Since each coil works independently, instead of excluding the data when one coil failed, *methods* were created to account for the missing data usually based on some type of linear interpolation. Other *corrections* were also developed to account for small heading errors, to center the keel on the sensor grid, and even to extrapolate the data to other depths. This process is commonly referred to as *gridding the data* and is often done based on what looks right, as opposed to what is physically realizable with emphasis given to the actual measured data.

The process of countering a ship's magnetic signature is based in large part on examining the difference of two runs. For example, the longitudinal component of the induced magnetic field of a ship requires the difference of a magnetic north run and a magnetic south run be computed, and, the effect of the onboard degaussing coils is determined by subtracting *coil-on* runs, from *coil-off* runs. Taking the difference of two runs, however, often exposes some of the difficulties associated with measuring underwater signatures, in particular, positioning and sensor orientation errors become more evident, and is the case for signature data created using the data gridding process.

In [1], a technique was developed to provide a realistic magnetic signature model based on; measurement data, a three-dimensional grid of magnetized prolate spheroids model, and a one-spike-at-a-time linear system inversion algorithm. The Magnetized Prolate Spheroid (MPS) model assumes the ship volume is filled with magnetized longitudinal prolate spheroids, each of which may have a magnetization in any or all of the orthogonal axes directions. From the physics, a linear system of equations is developed, which needs to be solved to determine the optimal magnetization weights (also referred to here as spikes) in the MPS model that best reproduce the measured magnetic field data, in a least-squares sense. A "spike" is defined as a single magnetization in one axis direction on one spheroid. Each spheroid in the model may have from zero (no magnetization at all) to three spikes. The one-spike-at-a-time algorithm was developed to return a sparsely populated magnetization weights solution to the inherently ill-conditioned linear system, that also fits to the measured magnetic field data. In [1], it is determined that the sparse weight solution returned from the one-spike-at-a-time algorithm is more physically realistic, compared to the Singular Value Decomposition (SVD) solution of minimum norm, and other algorithms, for modelling the source magnetizations of a ship, while still being able to solve the ill-conditioned system.

The first step of the modelling process is to align the sensor data to the ship and to determine the sensor position relative to the ship. With the introduction of affordable three-axis magnetometers many Navies are now changing to magnetic signature ranges using three-axis magnetometers collocated with three-axis accelerometers, and in Section 2.1 we describe how to orient the data to the ship's reference frame, as well as how to determine the sensor position relative to the ship. The wide spread use of GPS (Global Positioning System) tracking devices has also revolutionized how a vessel's position is determined and recorded, and in Section 2.2 we review how to determine a vessel's centroid position and heading from two GPSs mounted on the ship.

We then present an example where the MPS model and one-spike-at-a-time algorithm is used to model both a magnetic north run and a magnetic south run of *CFAV Quest*. The difference of the two runs is then computed to determine the vessel's induced longitudinal magnetic field.

2. Aligning magnetic field sensor data to a moving vessel

In a typical magnetic signature ranging of a vessel, magnetic field sensors are mounted on the seafloor in a line at some nominal spacing, and the vessel under test passes over the sensors perpendicular to the sensor line. The physical models which describe the ship's magnetic field however are usually in terms of the ship reference frame and for this reason the signature data is almost always required to be reoriented with respect to the ship.

In the underwater electromagnetic scientific community, most researchers have standardized on using the right handed rectangular coordinate system (x, y, z) shown in Fig. 1, where x is the ship's longitudinal axis with positive towards the bow, y is the ship's athwartship axis with positive in the starboard direction, and z is the vertical axis with positive downwards.

2.1 Orienting a collocated magnetometer and accelerometer sensor pair

A collocated three-axis magnetometer and three-axis accelerometer sensor pair provides, a relative acceleration vector[1] defined as $\boldsymbol{A}$, and a magnetic field vector $\boldsymbol{B}$ in three components. As is often the case we will reuse (x, y, z) for the sensor coordinates so that the relative acceleration vector can be described as

$$\boldsymbol{A} = \begin{bmatrix} A_x & A_y & A_z \end{bmatrix}^t, \tag{1}$$

[1] By convention, $\boldsymbol{A}$ is usually defined as the magnetic vector potential, but is used here to represent the relative acceleration vector.

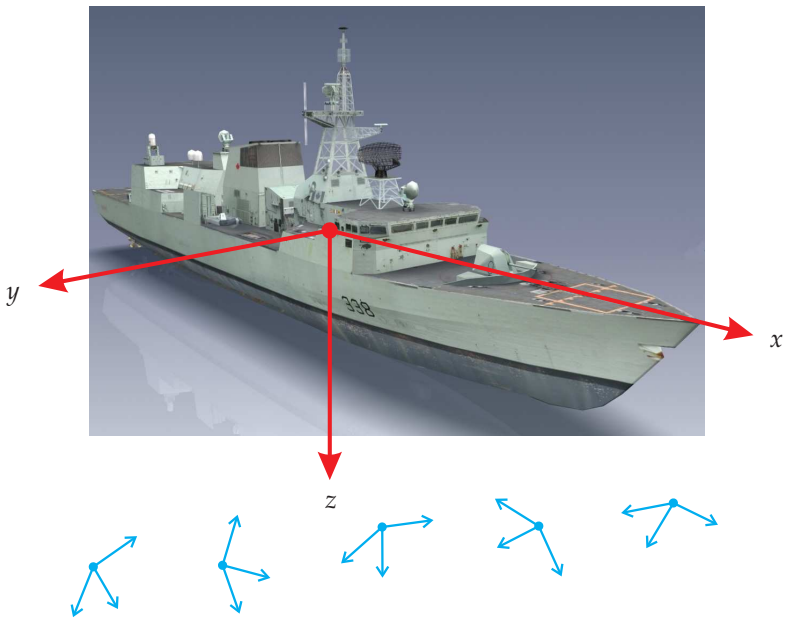

Figure 1: *Ship's coordinate system with three-axis magnetic field sensors mounted on the seafloor.*

and the magnetic field vector as

$$\boldsymbol{B} = \begin{bmatrix} B_x & B_y & B_z \end{bmatrix}^t, \tag{2}$$

where $\begin{bmatrix} \end{bmatrix}^t$ indicates the transpose. With this definition $\boldsymbol{A}$ and $\boldsymbol{B}$ are then column vectors, however, results here can be transposed to row vector form by exploiting the fact that $(\boldsymbol{RA})^t = \boldsymbol{A}^t\boldsymbol{R}^t$. We assume the sensor pair is stationary in the earth's gravitational field, and that the measured magnetic field is also constant and due only to the earth's magnetic field. To orient the collocated sensor pair, to a horizontal, vertical, and magnetic north reference frame, a roll, pitch and yaw set of rotation matrices can be used.

The standard definition of the roll, pitch and yaw model takes the form of three rotation matrices, one about each axis. Roll is defined as rotation about the x–axis and identified here by the roll angle ψ_x; pitch is defined as rotation about the y–axis and identified by the pitch angle ϕ_y; and yaw is rotation about the z–axis identified by the yaw angle θ_z. The rotation matrices are then

$$\boldsymbol{R}_x = \begin{bmatrix} 1 & 0 & 0 \\ 0 & \cos\psi_x & \sin\psi_x \\ 0 & -\sin\psi_x & \cos\psi_x \end{bmatrix}, \tag{3}$$

$$\boldsymbol{R}_y = \begin{bmatrix} \cos\phi_y & 0 & -\sin\phi_y \\ 0 & 1 & 0 \\ \sin\phi_y & 0 & \cos\phi_y \end{bmatrix}, \tag{4}$$

$$\boldsymbol{R}_z = \begin{bmatrix} \cos\theta_z & \sin\theta_z & 0 \\ -\sin\theta_z & \cos\theta_z & 0 \\ 0 & 0 & 1 \end{bmatrix}, \tag{5}$$

and must be applied in an order dependent manner. Positive rotation angles are directed along the positive rotation axis according to the right hand rule.

When levelling a collocated magnetometer/accelerometer sensor pair, the rotations are typically applied as roll, pitch, and then yaw. Thus, to level the data the rotation about the x–axis must bring the y–axis to horizontal (zero), and the second rotation about the new y–axis must bring the original x–axis to horizontal. The final rotation about the z–axis, which is now vertical, is typically done to zero the magnetic field of the y–axis, so that the x–axis is aligned to magnetic north.

It is possible to apply the rotations in a different order, however, the angles will change, and having the yaw angle last means it provides the sensor magnetic heading about a vertical z–axis. The order of the roll and pitch rotations could also be reversed, but offers no advantage and leads to rotations which are not in alphabetical order. The approach presented here is consistent with that used in [2].

More rigorously, we define the acceleration vector after the roll operation as $\boldsymbol{A}'$, and the acceleration vector after the pitch operation as $\boldsymbol{A}''$. The roll operation is then given as

$$\boldsymbol{A}' = \boldsymbol{R}_x \boldsymbol{A} \tag{6}$$

and leads to the following two equations in ψ_x

$$A'_y = A_y \cos\psi_x + A_z \sin\psi_x, \tag{7}$$
$$A'_z = -A_y \sin\psi_x + A_z \cos\psi_x. \tag{8}$$

Setting $A'_y = 0$ and solving for the roll angle ψ_x in Eqn. (7) yields

$$\psi_x = -\arctan\left(\frac{A_y}{A_z}\right), \tag{9}$$

where the four quadrant version of arctan is used. A roll angle of $\psi_x + 180^\circ$ will also achieve $A'_y = 0$, and typically the angle that yields a positive value for A'_z is used. After the roll rotation is applied, the relative acceleration vector becomes

$$\begin{bmatrix} A'_x \\ 0 \\ A'_z \end{bmatrix} = \boldsymbol{R}_x \begin{bmatrix} A_x \\ A_y \\ A_z \end{bmatrix}. \tag{10}$$

Since the roll rotation is about the x–axis, A_x remains unchanged so that $A'_x = A_x$, and, because $A'_y = 0$, A'_z is the vector sum of the two components A_y and A_z, such that

$$A'_z = \left(A_y^2 + A_z^2\right)^{1/2}. \tag{11}$$

The pitch operation is described as

$$\boldsymbol{A}'' = \boldsymbol{R}_y \boldsymbol{A}', \tag{12}$$

and leads to the following two equations in ϕ_y

$$A''_x = A'_x \cos\phi_y - A'_z \sin\phi_y, \tag{13}$$
$$A''_z = A'_x \sin\phi_y + A'_z \cos\phi_y. \tag{14}$$

To achieve $A''_x = 0$ requires a pitch angle ϕ_y given as

$$\phi_y = \arctan\left(\frac{A'_x}{A'_z}\right). \tag{15}$$

A pitch angle of $\phi_y + 180^\circ$ will also zero A''_x, and to achieve a downwards pointing result the angle that yields a positive value for A''_z is used. After the pitch rotation is performed the acceleration vector becomes

$$\begin{bmatrix} 0 \\ 0 \\ A''_z \end{bmatrix} = \boldsymbol{R}_y \begin{bmatrix} A'_x \\ 0 \\ A'_z \end{bmatrix}, \tag{16}$$

where

$$A''_z = \left({A'_y}^2 + {A'_z}^2 \right)^{1/2} = \left(A_x^2 + A_y^2 + A_z^2 \right)^{1/2}, \tag{17}$$

and should equal one if the original acceleration vector is a true relative acceleration with a magnitude of unity. Zero gravity is seen on the first two axes indicating they are horizontal.

We define $\boldsymbol{B}'$ as the magnetic field vector after both the roll and pitch operations have been applied such that

$$\boldsymbol{B}' = \boldsymbol{R}_y \boldsymbol{R}_x \boldsymbol{B}, \tag{18}$$

or in terms of field components

$$\begin{bmatrix} B'_x \\ B'_y \\ B_d \end{bmatrix} = \boldsymbol{R}_y \boldsymbol{R}_x \begin{bmatrix} B_x \\ B_y \\ B_z \end{bmatrix}, \tag{19}$$

where B_d is the required vertical down component. We define $\boldsymbol{B}''$ as the magnetic field after the yaw operation is performed such that

$$\boldsymbol{B}'' = \boldsymbol{R}_z \boldsymbol{B}', \tag{20}$$

and yields the following two equations in θ_z

$$B''_x = B'_x \cos\theta_z + B'_y \sin\theta_z, \tag{21}$$
$$B''_y = -B'_x \sin\theta_z + B'_y \cos\theta_z. \tag{22}$$

To orientate the first axis to magnetic north it is necessary that $B''_y = 0$ which requires a yaw angle θ_z of

$$\theta_z = \arctan\left(\frac{B'_y}{B'_x} \right), \tag{23}$$

and yields for the final magnetic field vector

$$\begin{bmatrix} B_n \\ 0 \\ B_d \end{bmatrix} = \boldsymbol{R}_z \boldsymbol{R}_y \boldsymbol{R}_x \begin{bmatrix} B_x \\ B_y \\ B_z \end{bmatrix}. \tag{24}$$

Where $B''_x = B_n$ is the magnetic north component of the magnetic field, and $B''_y = B_e$ is the magnetic east component and equals zero since the axes are now aligned to magnetic north.

We now have a level magnetic field vector and B_d is the required vertical down magnetic component and is therefore coincident with the ship's vertical field B_z defined in Fig. 1. Resolving the horizontal components of the magnetic field to the ship's axis is discussed next.

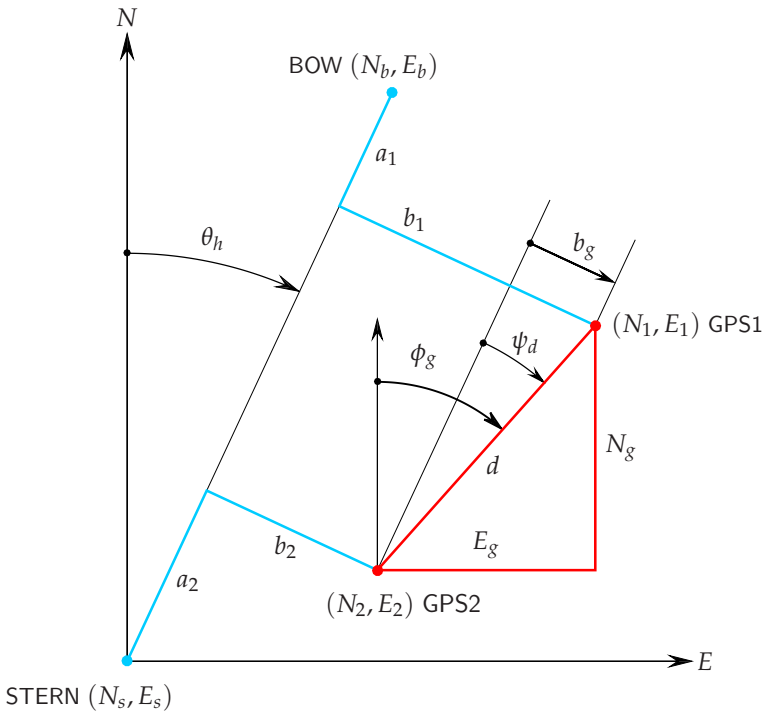

Figure 2: *Two GPSs on ship offsetted the from bow and stern.*

2.2 Two GPSs offsetted from the bow and stern

When a vessel is tracked with two GPSs, it is often the case that the GPSs are not located at the exact bow and stern position. For our modelling purposes, the ship's heading is defined here as θ_h, and the ship's length L. The ship's centroid position, in terms of a northing and easting value (N, E) are required, and can be easily calculated once the bow and stern locations are determined. This section derives the bow and stern locations from two GPSs mounted at some arbitrary location on the vessel, and then provides solutions for the ship's heading, length and position.

To determine the bow and stern positions in terms of the measured GPSs locations, consider Fig. 2, where we define the bow and stern positions in terms of their northing and easting position, as (N_b, E_b) and (N_s, E_s), respectively. The GPS positions are given as (N_1, E_1) and (N_2, E_2), and are defined with respect to the bow and stern by the ordered pairs (a_1, b_1) and (a_2, b_2), which are measured along the vessel's longitudinal and athwartship axes.

The differences between the two GPS locations defined as N_g and E_g can be calculated as

$$N_g = N_1 - N_2, \tag{25}$$

and

$$E_g = E_1 - E_2, \tag{26}$$

and used to determine a GPS heading defined as ϕ_g, and given as

$$\phi_g = \arctan\left(\frac{E_g}{N_g}\right), \tag{27}$$

where arctan is understood to return the correct four quadrant result by checking the signs of N_g and E_g. The distance between the GPSs is defined as d and given as

$$d = \left(N_g^2 + E_g^2\right)^{1/2}. \tag{28}$$

The athwartship offset between the two GPSs is defined as b_g and is determined as

$$b_g = b_1 - b_2, \tag{29}$$

and is negative when GPS1 is to the port side of GPS2. In Fig. 2, all variables have been drawn with positive values, to assist in deriving a four quadrant result. The GPS offset angle to the ship's heading, defined as ψ_d, can be determined as

$$\psi_d = \arcsin\left(\frac{b_g}{d}\right), \tag{30}$$

and has the same sign as b_g. The ship's heading is calculated as

$$\theta_h = \phi_g - \psi_d, \tag{31}$$

and once known, allows the bow position to be determined as

$$N_b = N_1 + a_1 \cos\theta_h + b_1 \sin\theta_h, \tag{32}$$
$$E_b = E_1 + a_1 \sin\theta_h - b_1 \cos\theta_h, \tag{33}$$

and the stern position as

$$N_s = N_2 - a_2 \cos\theta_h + b_2 \sin\theta_h, \tag{34}$$
$$E_s = E_2 - a_2 \sin\theta_h - b_2 \cos\theta_h. \tag{35}$$

Which can be represented in matrix notation as

$$\begin{bmatrix} N_b \\ E_b \end{bmatrix} = \begin{bmatrix} N_1 \\ E_1 \end{bmatrix} + \begin{bmatrix} \cos\theta_h & \sin\theta_h \\ \sin\theta_h & -\cos\theta_h \end{bmatrix} \begin{bmatrix} a_1 \\ b_1 \end{bmatrix}, \tag{36}$$

and

$$\begin{bmatrix} N_s \\ E_s \end{bmatrix} = \begin{bmatrix} N_2 \\ E_2 \end{bmatrix} - \begin{bmatrix} \cos\theta_h & -\sin\theta_h \\ \sin\theta_h & \cos\theta_h \end{bmatrix} \begin{bmatrix} a_2 \\ b_2 \end{bmatrix}, \tag{37}$$

where the (2×2) matrices are known as transformation matrices.

The ship's heading can be recalculated as

$$\theta_h = \arctan\left(\frac{E_b - E_s}{N_b - N_s}\right), \tag{38}$$

and confirmed with the result above. The ship's centroid position is taken as the average of the bow and stern positions so that

$$N = \frac{N_b + N_s}{2}, \tag{39}$$

and

$$E = \frac{E_b + E_s}{2}. \tag{40}$$

The length of the ship L can now be calculated as

$$L = \left[(N_b - N_s)^2 + (E_b - E_s)^2\right]^{1/2}, \tag{41}$$

and compared to a known amount as an estimate of the positioning error.

2.3 Sensor position with respect to the ship

For modelling purposes, both the signature data and the sensor position must be determined in the ship's coordinate system. For this section we use the ship's coordinate system (x, y, z) as defined earlier in Fig. 1, but now use (u, v, w) for the sensor to distinguish the two.

If the sensor data has been leveled and aligned to some geographic reference as described in Section 2.1, then the w–axis is vertical and coincident with the z–axis of the vessel. This leaves the two dimensional problem which is depicted in Fig. 3 where the ship is at some position (N, E) with some heading θ_h and the sensor is considered vertical on the seafloor with its (u, v) axis oriented at some angle ϕ_s from the ship's heading.

For the sensor data all that is required is that the data in the (u, v) sensor coordinate system be rotated to the (x, y) ship coordinate system by the required rotation angle, which has been defined as ϕ_s. The magnetic field values in ship's coordinates are then given as

$$\begin{bmatrix} B_x \\ B_y \\ B_z \end{bmatrix} = \begin{bmatrix} \cos\phi_s & \sin\phi_s & 0 \\ -\sin\phi_s & \cos\phi_s & 0 \\ 0 & 0 & 1 \end{bmatrix} \begin{bmatrix} B_u \\ B_v \\ B_w \end{bmatrix}. \tag{42}$$

If the u–axis has been oriented to magnetic north, as described in Section 2.1, then the required rotation ϕ_s would be considered the ship's magnetic heading and given as $\phi_s = \theta_h - \theta_m$ where θ_m is the local magnetic declination. Interestingly, despite having a number of magnetometers deployed the local magnetic declination must be determined separately with surveying apparatus. The magnetic sensors can determine the angles to rotate the sensors to magnetic north, but not where magnetic north is relative to true north. For the example in Fig. 3 the local magnetic declination θ_m has been drawn with a negative value.

To determine the sensor position with respect to the ship, we first determine the northing and easting distances to the ship from the sensor, defined as N_s and E_s respectively, and calculated as

$$N_s = N - N_0, \tag{43}$$

and

$$E_s = E - E_0, \tag{44}$$

where (N_0, E_0) is the sensor position and is assumed to be stationary. For the example shown in Fig. 1, the ship is positioned to the southwest of the sensor and both N_s and E_s, as shown, are less than zero. To determine the position of the sensor relative to the ship, that is the (x, y) values describing the sensor position, the N_s and E_s distance vectors are projected along the ship's longitudinal and athwartships axes to yield

$$x = -N_s \cos\theta_h - E_s \sin\theta_h, \tag{45}$$
$$y = N_s \sin\theta_h - E_s \cos\theta_h, \tag{46}$$

or

$$\begin{bmatrix} x \\ y \end{bmatrix} = \begin{bmatrix} -\cos\theta_h & -\sin\theta_h \\ \sin\theta_h & -\cos\theta_h \end{bmatrix} \begin{bmatrix} N_s \\ E_s \end{bmatrix}. \tag{47}$$

For the example in Fig. 1 the ship is considered to be approaching the sensor from the southwest (e.g. at the start of a pass) so that in ship's coordinates both x and y are greater than zero as shown. If the course is maintained, as the ship passes over the sensor, the value of x will decrease to zero at the closest point of approach (CPA), and then go negative as the ship passes by; whereas the value of y will stay constant and positive since the sensor will remain a constant distance off the ship's starboard side.

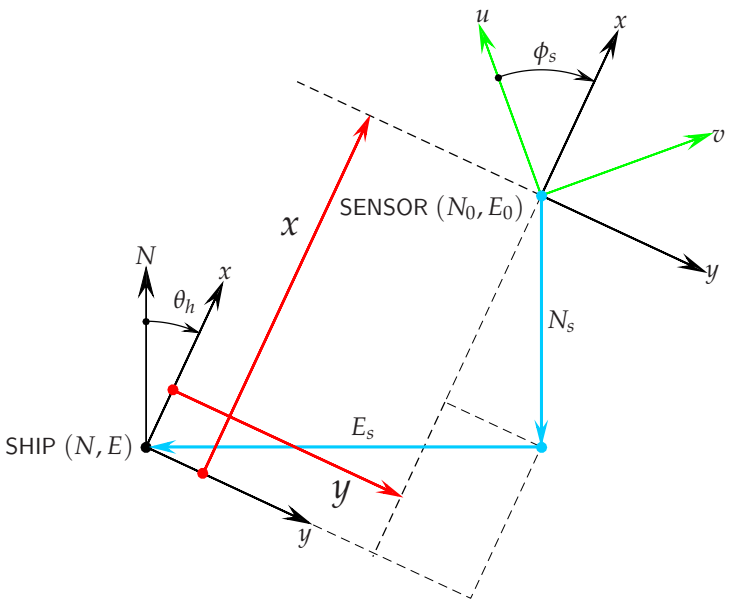

Figure 3: *Sensor position relative to ship.*

3. Magnetic ranging example

On November 21, 2011 *CFAV Quest* conducted a magnetic signature ranging at the Bedford Basin Degaussing Range located in Halifax, Nova Scotia, Canada. Two of the runs collected during that trial are analyzed here to demonstrate how the one-spike-at-a-time method can be used to model the vessel's magnetic signature of a particular run and then how the difference of two runs can be used to calculate the induced longitudinal field of the vessel.

3.1 Modelling the magnetic signature of a single pass

To use the one-spike-at-a-time model the data must be referenced to the passing vessel and the position of the sensor relative to the ship determined. The magnetic range at Bedford Basin has sixteen three-axis induction coils and Fig. 4 shows data from five of the sixteen three-axis sensors for a north bound run. The sensor positions (x, y, z) are plotted in the lower panel and the corresponding magnetic field vector components (B_x, B_y, B_z) are shown in the upper panel, all relative to the ship, as required. This data set has undergone the gridding process described above but is still useful for demonstrating modelling concepts.

The sensor positions (x, y, z), as shown in Fig. 4 have all been concatenated together into long vectors for each axis. For each sensor the value of x begins positive, then decreases to zero, and then goes negative indicating the vessel passed over the sensor. The y value is essentially constant for each sensor indicating a constant heading, and each successive value varies by the sensor separation. All the z values for all sensors are approximately the same since each sensor has been mounted at about the same depth.

The one-spike-at-a-time algorithm populates the magnetizations of a three-dimensional grid of magnetized longitudinal prolate spheroids in the MPS model by determining the most dominate spike (magnetization weight and spheroid location) that reduces the RMS error between the measured and model data the most, and then forces that spike *location* to be included in the final solution. The entire linear system is then

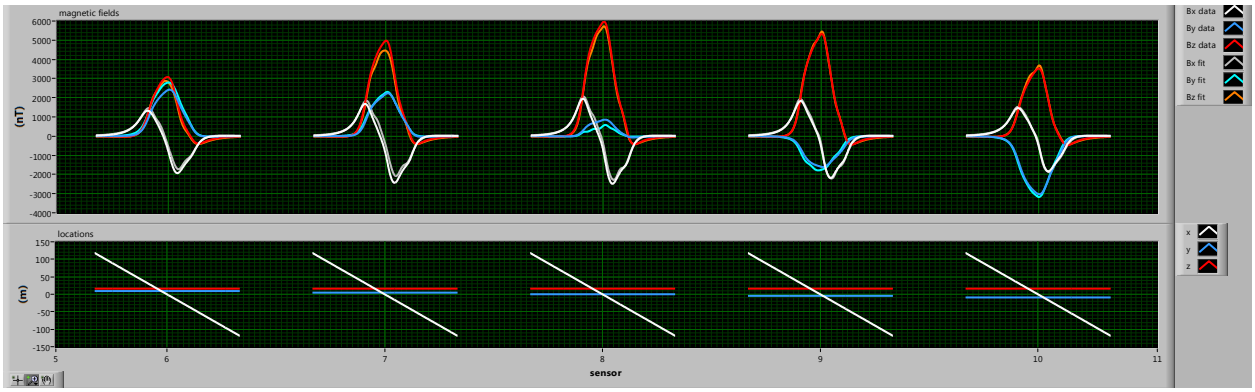

Figure 4: *Measured and modelled magnetic signature data, and sensor positions relative to the ship. The longitudinal* (x) *components are shown in white, the athwartship* (y) *components in blue, and the vertical* (z) *components in red.*

orthogonalized with respect to this spike location. A new search is then started for the next dominant spike location and weight (excluding any previously determined locations) that again reduces the RMS error the most. The weight of this new spike and any previous spike(s) are allowed to vary, but the locations are not. This iterative process is then repeated until enough spikes have been included into the model such that the RMS error of the fit is converging to a reasonable value, and the magnetization weights in the solution have not started to oscillate. If oscillations in the solution weights are occurring, then too many spikes have been included into the model. Oscillations occur when effectively some near-zero singular values of the model matrix are being used in the solution for the weights. Whereas the number of possible magnetic weights might be in excess of several hundred, the one-spike-at-a-time algorithm identifies the most dominate twenty-or-so spikes to fit the data, with all the remaining possible spheroid magnetizations having zero weight.

To support the rapid visualization of the MPS model and the resulting magnetic signature, DRDC is developing a NI LabVIEW [3] application known as TURNS Vector Visualization using 1-Spike-at-a-Time Regularization (TW1STR). The project is in support of the Transportable Underwater Range for Naval Signatures (TURNS) portable magnetic range being built for the Royal Canadian Navy as part of the Halifax Class Modernization. Figs. 4–10 are all produced directly from the TW1STR application.

Fig. 5 displays the grid of prolate spheroids created to model the *CFAV Quest* data set. The spheroids are arranged throughout the ship volume and include one spheroid set to the approximate size of the vessel, and is included or not in the final solution in the same manner as any of the other magnetizations.

The MPS model and one-spike-at-a-time algorithm is able to fit the gridded data in the north run example shown in Fig. 4, to an error of 9.3 % using only 15 of the available 375 magnetic moments in the model. The fitting errors for the individual field components were 13.7 %, 10.0 % and 7.0 % for (x, y, z) respectively. Fig. 4 shows both the original data and the fitted data obtained by the model for each component. The 15 magnetic moments are plotted using a three dimensional perspective view in Fig. 6 revealing the moment locations, which for *CFAV Quest* are dominated by downward pointing vertical magnetization.

Once a model with an acceptable fitting error and realistic magnetic moments has been created the magnetic signature can now be generated anywhere in space. Often the data is plotted at a depth equal to the vessel's beam or some other standard depth, or even above the ship if the anomaly from an aircraft was of interest. For the *CFAV Quest* data set just modelled the individual field components are plotted in Fig. 7

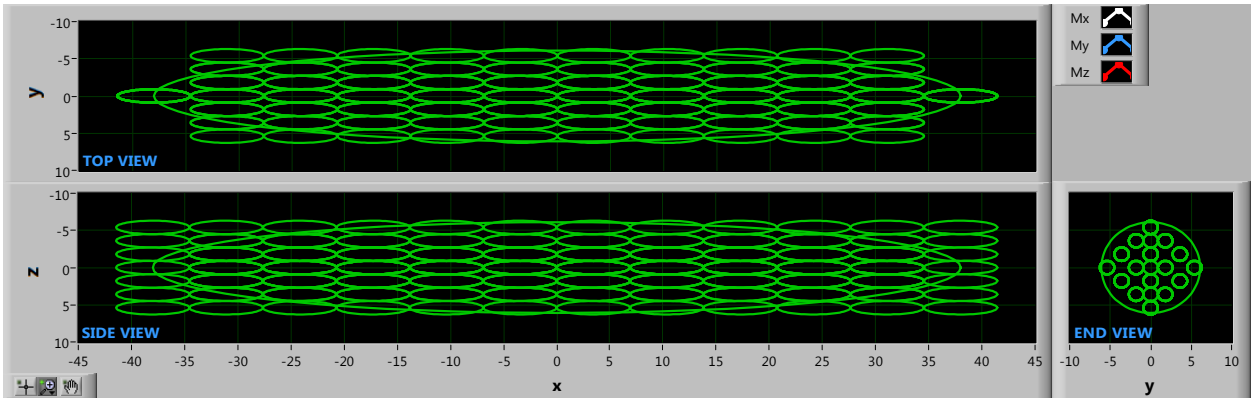

Figure 5: *Locations of the longitudinal prolate spheroids which includes a spheroid approximately the vessel size.*

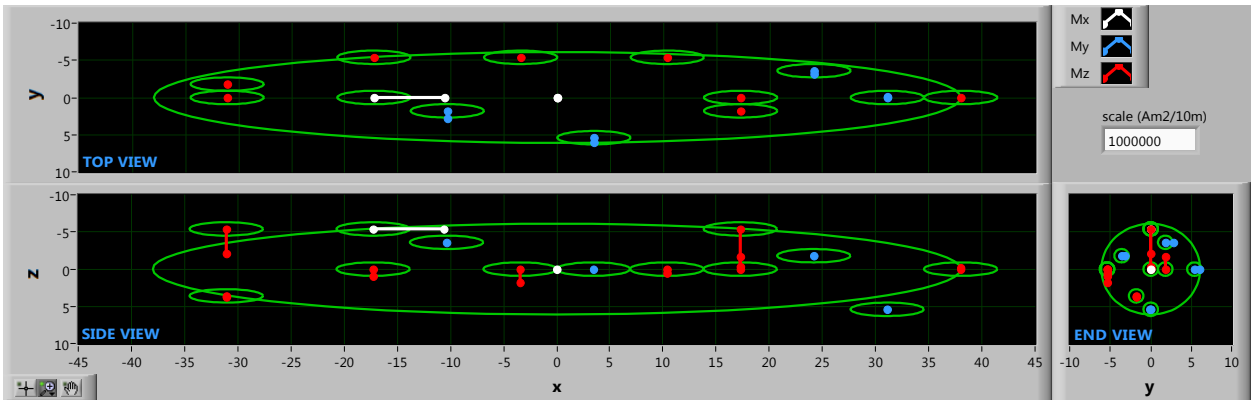

Figure 6: *Location and strength of the* 15 *magnetic moments used to fit the north bound run.*

on the grid:

$$\begin{aligned} -100\,\mathrm{m} \leq & x \leq 100\,\mathrm{m}, \quad \Delta x = 4\,\mathrm{m} \\ -50\,\mathrm{m} \leq & y \leq 50\,\mathrm{m}, \quad \Delta y = 4\,\mathrm{m} \end{aligned}$$

at a depth of $z = 20\,\mathrm{m}$. The peak vertical magnetic field is observed to be about 4000 nT, and is typical for a vessel this size with no magnetic treatment or degaussing.

The magnetic signature of *CFAV Quest* is in fact consistent with the signature of many vessels which have spent their working life in the northern hemisphere, and that have never undergone magnetic treatment, in that, the signature possesses the following attributes:

$$\begin{aligned} B_x > 0 \quad \text{when} \quad x > 0, \\ B_y > 0 \quad \text{when} \quad y > 0, \\ B_z > 0 \quad \text{when} \quad z > 0, \end{aligned}$$

which are indicative of a vessel with a downwards pointing magnetization, which in this case was brought about due to long term exposure in the earth's downward pointing magnetic field in the northern hemisphere.

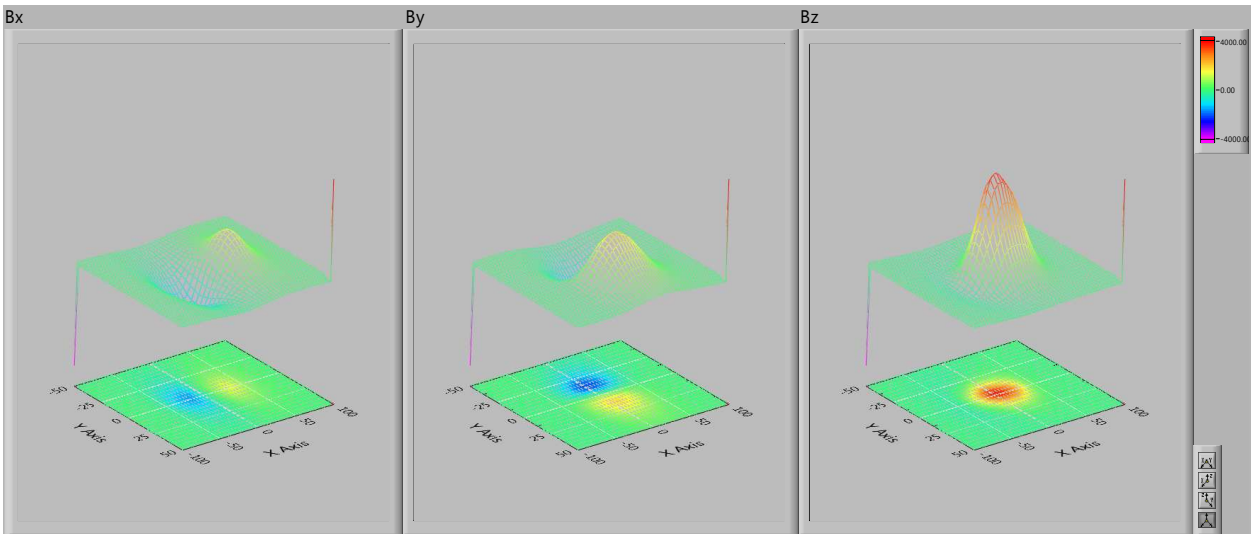

Figure 7: *Modelled north bound magnetic signature at* 20 m *depth.*

3.2 Over-fitting the magnetic signature

If the number of spikes are increased to 75, for example, the overall fitting error decreases to 9.3 % and the component errors to 13.1 %, 9.3 % and 6.7 %. As is evident by the modest error reduction increasing the number of spikes does not significantly improve the fitting error. What does occur is the moments estimated become excessively large and oscillatory in space as seen in Fig. 8 for the 75 moment solution. While adding spikes always decreases the error, the key to the process is choosing an appropriate number of moments to fit the data without the moments becoming unrealistically large and oscillatory.

3.3 Removing interpolated data

At the time of the magnetic field measurements of *CFAV Quest*, sensor units 2, 4, 7, 8 and 13 at the degaussing range had at least one malfunctioning channel, and the missing sensor data has been estimated and inserted into the data set using interpolation of adjacent sensor channels from functioning sensors. If this interpolated data is excluded from the modelling procedure, so that, only real measured data is used, we find that just 8 moments can fit the data with an overall error of just 8.6 %, with component errors of 12.5 %, 11.4 % and 6.0 %. This indicates that the inserted data is not physically consistent with the measured data, since the error increases when it is used. Even the location and strength of the moments shown in Fig. 9 are more physically consistent, suggesting now, both a dominate vertical magnetization and a positive athwartship magnetization along the starboard side of the ship.

3.4 Calculation of the longitudinal induced magnetic signature

The reciprocal south bound run was modelled in a similar fashion, and due to the large permanent magnetization present in the vessel was similar in magnitude and structure to the north bound run. The average of the two runs is the permanent (or constant) signature and half the difference is the longitudinal induced magnetic signature which is shown in Fig. 10, using the same grid as above. The peak vertical induced magnetic field is about 900 nT, or about 22 % of the total signature.

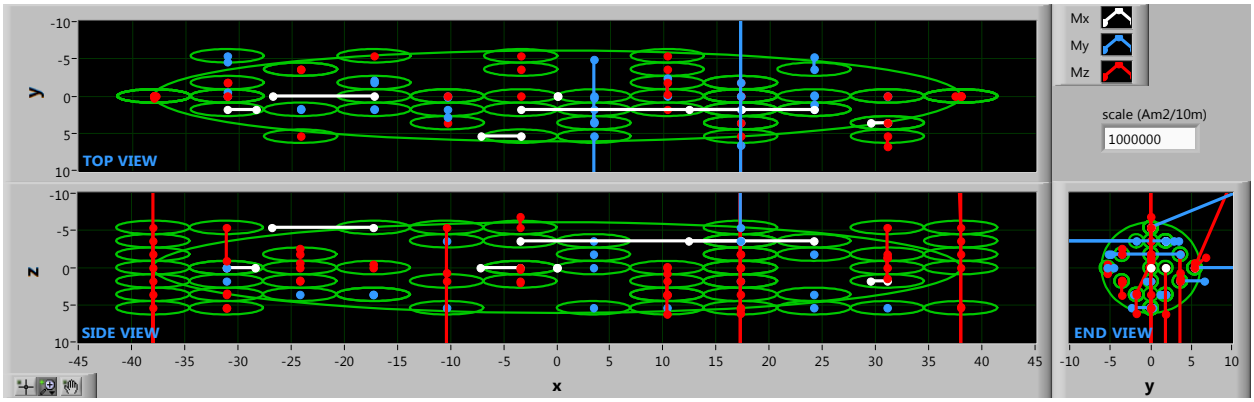

Figure 8: *Location and strength when* 75 *magnetic moments are used to fit the north bound run.*

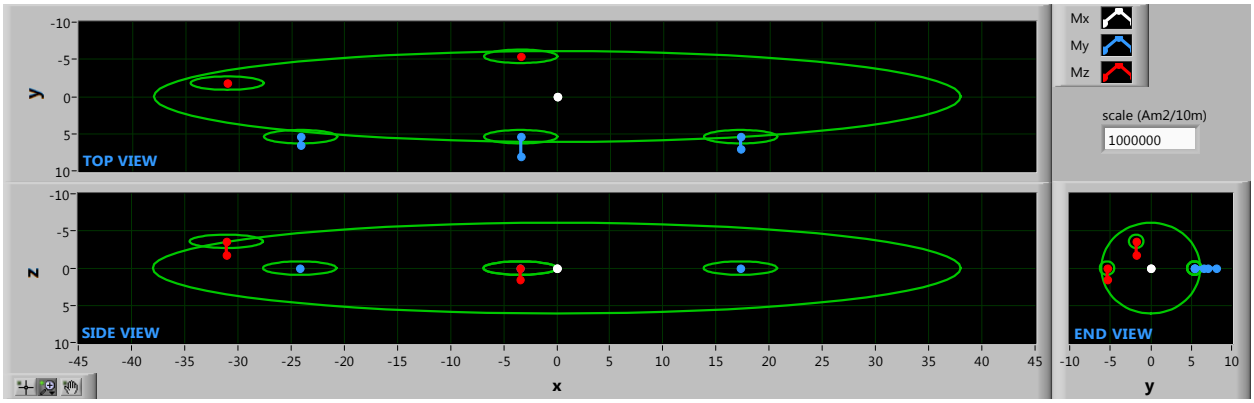

Figure 9: *Location and strength when* 8 *magnetic moments are used to fit the north bound run, with no interpolated data used.*

4. Conclusions

We have introduced a novel technique for modelling and viewing a ship's magnetic signature. The modelling process requires taking measured magnetic field data obtained from a moving ship by underwater sensors and transforming this data into a spatial coordinate system relative to the ship. A procedure was outlined for orienting collocated magnetometer and accelerometer sensor pairs used to collect ship magnetic data, using the earth's gravitational and magnetic fields to align the sensors to horizontal and magnetic north. A detailed procedure to localize a ship using bow and stern mounted GPS receivers was developed for the modelling process, which also determines the sensor positions with respect to the ship. The magnetic fields of the ship are modelled using a Magnetized Prolate Spheroid model and a novel one-spike-at-a-time inversion algorithm is used to determine the three-dimensional distribution of magnetization weights that model the measured data. A LabVIEW application was developed for rapid modelling and viewing of the measured data and modelling results.

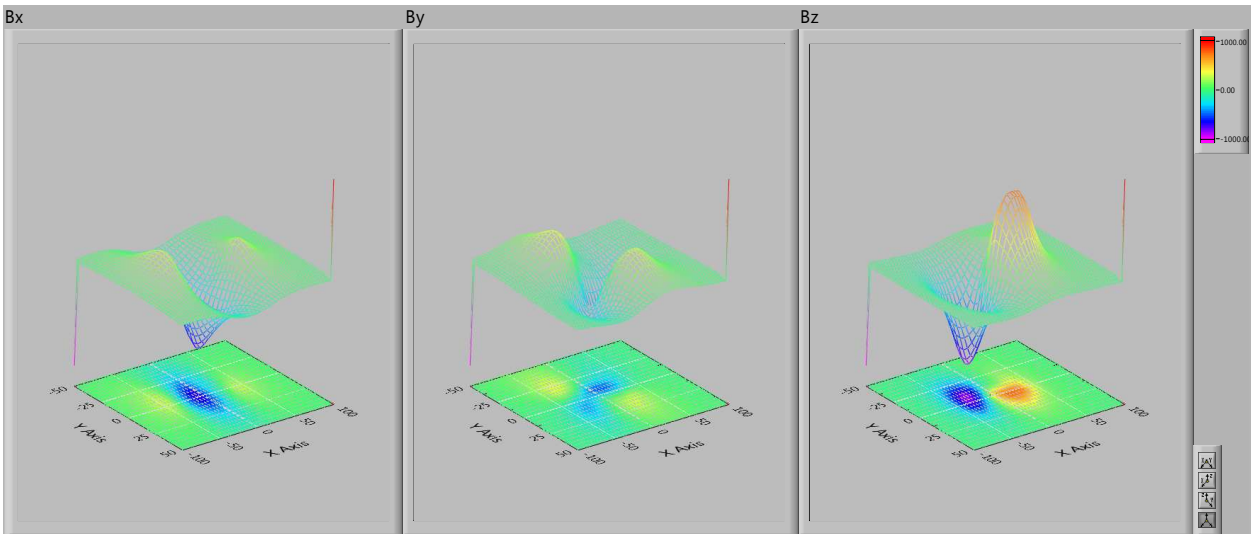

Figure 10: *Modelled longitudinal induced magnetic signature at* 20 m *depth.*

Acknowledgements

We would like to thank Dr. Peter Holtham (retired) for initiating the magnetic modelling research at the Defence Research Establishment Pacific (DREP), and for his hard work and guidance. We would also like to thank Dr. Ian Barrodale of Barrodale Computing Services Ltd. for his original work in developing the one-spike-at-a-time inversion algorithm.

References

[1] Peter M. Holtham and Carmen E. Lucas. New approaches to magnetic modelling i. prolate spheroids ii. one-spike-at-a-time fitting. Technical Report 93-81, Defence Research Establishment Pacific, 1993.

[2] Sparton Electronics. *SPARTON SP3003D DIGITAL COMPASS*. Sparton, Schaumburg, IL, USA, 2006.

[3] National Instruments ©. *LabVIEW development system*. National Instruments Corporation, Austin, TX, USA, 2015.